

Charge Transfer Complexes Beneficial Method for Determination of Fluoxetine HCl Pure Drug: Spectroscopic and Thermal Analyses Discussions¹

Abeer A. El-Habeeb^a and Moamen S. Refat^{b,c}

^a Department of Chemistry, Faculty of Science, Princess Nora Bint Abdul Rahman University, Riyadh, Kingdom Saudi Arabia

^b Department of Chemistry, Faculty of Science, Port Said, Port Said University, Egypt

^c Department of Chemistry, Faculty of Science, Taif University, Al-Haweiah, P.O. Box 888, Zip Code 21974, Taif, Saudi Arabia
e-mail: msrefat@yahoo.com

Received July 13, 2014

Abstract—A simple and conventional spectrophotometric method is developed for quantitative analysis of fluoxetine. The method is based on the charge transfer 1 : 1 complex formation of fluoxetine hydrochloride with electron acceptors: picric acid, dinitrobenzene, *p*-nitrobenzoic acid, 2,6-dichloroquinone-4-chloroimide, 2,6-dibromoquinone-4-chloroimide and 7,7',8,8'-tetracyanoquinodimethane. The charge-transfer complexes are isolated and characterized by elemental analysis, conductivity, IR, Raman, ¹H NMR spectra, X-ray powder diffraction, scanning electron microscopy and thermogravimetric analysis. The formation constants (K_{CT}), molar extinction coefficients (ϵ_{CT}), standard free energies (ΔG^0), oscillator strengths (f), dipole moments (μ), resonance energies (R_N) and ionization potentials (I_D) are estimated. Thermodynamic parameters were computed from the thermal decomposition data.

Keywords: fluoxetine hydrochloride; *n*-donor; π -acceptors; IR, Raman, NMR spectroscopy; charge transfer complexes; thermogravimetric analysis

DOI: 10.1134/S1070363214090291

INTRODUCTION

Fluoxetine {FXN, (*RS*)-*N*-methyl-3-phenyl-3-[4-(trifluoromethyl)phenoxy]propan-1-amine} is used for the treatment of major depressive disorder, obsessive-compulsive disorder, bulimia nervosa, panic disorder and premenstrual dysphoric disorder [1]. FXN has been determined in its drug formulations using titrimetry [2], ¹H and ¹³C NMR spectroscopy [3], potentiometric analysis [4], liquid [5] and gas chromatography [6], and electrophoresis [7]. These methods are time-consuming and expensive analytical instruments. Spectrophotometric and fluorimetric methods [8, 9] are the most convenient techniques because of their simplicity and low cost.

Charge-transfer (CT) complexation is an important phenomenon in biochemical and bioelectrochemical energy transfer processes [10]. CT interactions

between electron donors and acceptors are generally associated with the formation of intensely colored CT complexes [11]. Molecular complexation and structural recognition are important processes in biological systems; for example, drug action, enzyme catalysis, and ion transfers through lipophilic membranes all involve complexation [12]. The CT complexation is an important technique that is cheaper, simpler, and more efficient than the methods of drug determination described in the literature [13–21].

The CT products of FXN with picric acid (PA), dinitrobenzene (DNB), *p*-nitro-benzoic acid (*p*-NBA), 2,6-dichloroquinone-4-chloroimide (DCQ), 2,6-dibromo-quinone-4-chloroimide (DBQ) and 7,7',8,8'-tetracyanoquinodimethane (TCNQ) have not yet been studied in the literature; therefore the aim of the present study was to investigate the spectroscopic and thermal behavior of these CT interactions. The spectrophotometric tool using molar ratio method is successful in determining the FXN pure drug by the

¹ The text was submitted by the authors in English.

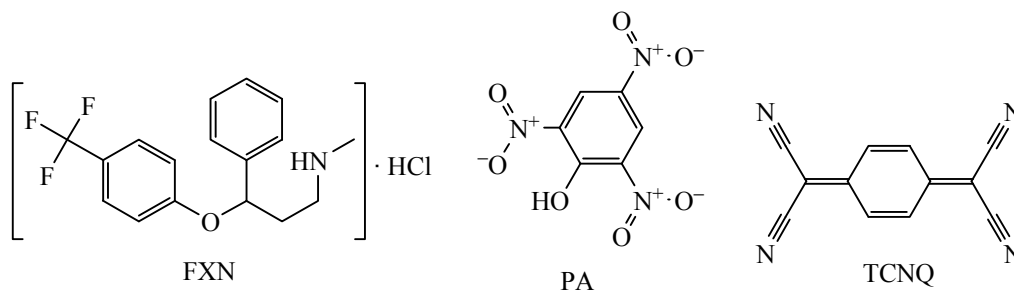


Fig. 1. Fluoxetine hydrochloride (FXN) and π -acceptors: PA and TCNQ.

formation of the CT complexes with the six π -electron acceptors through π - π and/or n - π transitions.

EXPERIMENTAL

Materials. All chemicals and reagents used in this study were of analytical grade. Fluoxetine hydrochloride was obtained from Egyptian International Pharmaceutical Industries Company. PA, DNB, *p*-NBA, DCQ, DBQ, and TCNQ were obtained from Aldrich and Fluka Chemical Companies (Fig. 1).

Synthesis of solid FXN charge transfer complexes. Six Fluoxetine hydrochloride solid CT complexes with PA (dark yellow), DNB (white), *p*-NBA (white), DCQ (brown), DBQ (dark brown) and TCNQ/FXN (light green) were synthesized by mixing (1 mmol, 0.31 g) of fluoxetine hydrochloride in 20 mL methanol to 1 mmol of the acceptor in 20 mL

chloroform. All mixtures were stirred for 1 h at room temperature, the solid products were filtered off, washed with minimum amounts of chloroform and dried under vacuum over anhydrous CaCl_2 .

Physical and analytical measurements. The elemental analysis on C, H, N was performed using a Perkin Elmer CHN 2400. The molar conductivities of freshly prepared 1.0×10^{-3} mol/cm³ DMSO solutions were measured on a Jenway 4010 conductometer. The electronic absorption spectra were recorded in methanol within 800–200 nm range using a Perkin-Elmer Precisely Lambda 25 UV/Vis double beam Spectrometer fitted with a quartz cell of 1.0 cm path length. IR spectra in the range 4000–400 cm⁻¹ for the free reactants and the CT complexes were recorded in KBr on a Shimadzu FT-IR Spectrometer with 30 scans and 2 cm⁻¹ resolution, while Raman spectra were

Table 1. Physical and analytical data of FXN charge transfer complexes

Compound (M_w)	Color (before ppt)	Color (after ppt)	Λ_m , ($\Omega^{-1}\text{cm}^{-1}\text{mol}^{-1}$)	Elemental analysis						Yield, %
				found, %			calculated, %			
				C	H	N	C	H	N	
FXN (345.79)	–	White	9	59.05	5.54	4.05	58.89	5.43	3.97	–
[(FXN)(PA)] (574.89)	Yellow	Dark yellow	50	48.05	3.86	9.75	47.92	3.77	9.45	65
[(FXN)(DNB)] (513.89)	Colorless	White	37	53.76	4.51	8.18	53.22	4.34	8.02	72
[(FXN)(<i>p</i> -NBA)] (512.91)	Colorless	White	56	56.20	4.72	5.46	55.89	4.66	5.41	70
[(FXN)(DCQ)] (556.23)	Brown	Brown	41	49.66	3.81	5.04	49.13	3.65	4.87	69
[(FXN)(DBQ)] (645.13)	Brown	Dark brown	43	42.82	3.28	4.34	42.74	3.19	4.23	71
[(FXN)(TCNQ)] (539.97)	Green	Light green	49	63.33	4.22	12.73	63.02	4.08	12.43	66

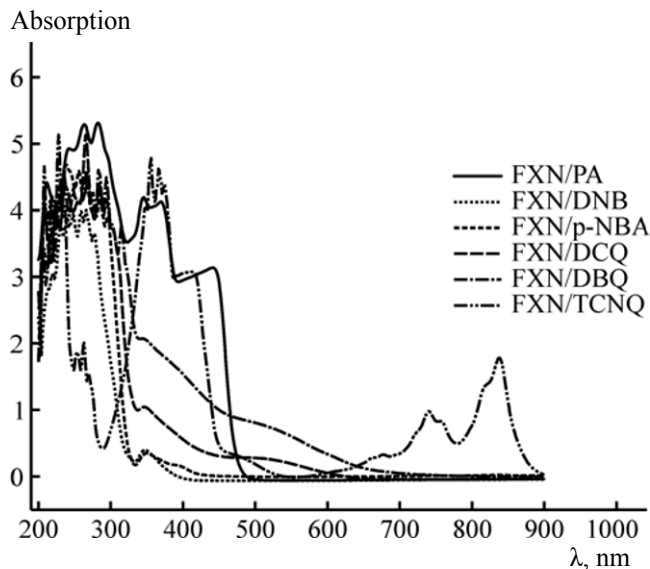


Fig. 2. Electronic absorption spectra of the CT complexes in methanol solution.

measured on a Bruker FT-Raman with laser 50 mW. ^1H NMR spectra were recorded on a Bruker 600 MHz spectrometer in DMSO with TMS as an internal standard. DTG-TG thermograms were obtained on a Shimadzu TGA-50H. Solid samples were placed in platinum pans with a pierced lid, and heated with the rate of $30^\circ\text{C}/\text{min}$ under nitrogen flow. Scanning electron microscopy (SEM) images and Energy Dispersive X-ray Detection (EDX) were taken on a Joel JSM-6390 instrument, with the accelerating voltage 20 kV. X-ray diffraction patterns were recorded on a Bruker Advanced 8 X-ray powder diffraction, CuK_α radiation, step scan mode with step = 0.05° and counting time 3.0 sec/step.

RESULTS AND DISCUSSION

Analytical and physical measurements. The results of analysis (molecular weights, molecular formula, conductivity, yield, color before and after precipitation, composition) of all FXN complexes are listed in Table 1. As can be seen, the experimental values are in a good agreement with the theoretical data and the formulae of the CT complexes are compatible with the molar ratios which were obtained from the photometric titration curves of FXN with electron π -acceptors. The elemental analysis proves the 1 : 1 composition of the complexes. The complexes are insoluble in water, partly soluble in alcohols, but easily soluble in dimethylformamide (DMF) and dimethylsulfoxide (DMSO).

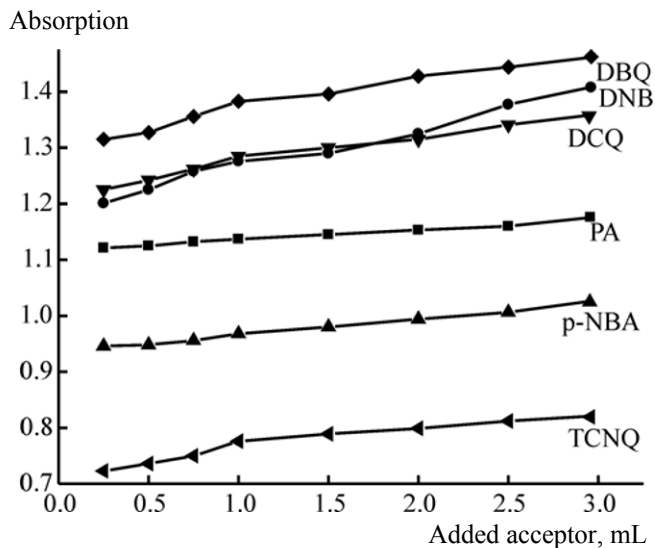


Fig. 3. Photometric titration spectra of the CT complexes at the CT peaks.

Molar conductivity measurements. The molar conductivities of FXN CT complexes and free reactants were measured for DMSO solutions of $1.0 \times 10^{-3} \text{ mol/dm}^3$ concentration. The measured values fall in the range $37\text{--}56 \Omega^{-1} \text{ cm}^2 \text{ mol}^{-1}$ indicating a slightly electrolytic nature of the CT complexes with the hydrogen bond between the lone pair of the nitrogen atom and the slightly positive hydrogen atom in the molecule of acceptor [22].

Electronic spectra and spectroscopic parameters. The electronic spectra of PA, DNB, *p*-NBA, DCQ, DBQ and TCNQ/FXN CT complexes were measured in CH_3OH solvent. The complexes were formed by adding $X \text{ mL}$ of $5.0 \times 10^{-4} \text{ M}$ (PA, DNB, *p*-NBA, DCQ, DBQ, or TCNQ) where ($X = 0.25, 0.50, 0.75, 1.00, 1.50, 2.00, 2.50$, and 3.00 mL) to 1.00 mL of $5.0 \times 10^{-4} \text{ M}$ FXN. The total volume of each system was completed to 5 mL with methanol solvent. The FXN concentration in the reaction mixture was kept fixed at $1.00 \times 10^{-4} \text{ M}$ in CH_3OH solvent, while the concentration of the π -acceptor varied from $0.25 \times 10^{-4} \text{ M}$ to $3.00 \times 10^{-4} \text{ M}$. The electronic absorption spectra of the complexes are shown in Fig. 2.

The spectra of the CT complexes contain absorption bands which are lacking in the spectra of free reactants. These bands appear at 441, 348, 395, 516, 531, and 412 nm for the CT complexes of FXN with PA, DNB, *p*-NBA, DCQ, DBQ or TCNQ, respectively. Photometric titration curves obtained by the

known technique [23] are given in Fig. 3. The equivalence points shown in these curves clearly indicate that the formed CT complexes between FXN and all π -acceptors are 1 : 1. Note, that the solvent has a pronounced effect on association of the formed [(FXN)(π -acceptors)] complexes.

The modified Benesi-Hildebrand equation [24] was used in the calculations

$$\frac{C_a^0 C_d^0 I}{A} = \frac{1}{K\varepsilon} + \frac{C_a^0 + C_d^0}{\varepsilon}, \quad (1)$$

where C_a^0 and C_d^0 are the initial concentrations of the acceptor and the donor, respectively, K is complexation constant, ε is molar extinction coefficient, and A is the absorbance of bands at 441, 348, 395, 516, 531, and 412 nm for complexes with PA, DNB, *p*-NBA, DCQ, DBQ, and TCNQ. The $C_a^0 C_d^0 / A$ values plotted against $C_a^0 + C_d^0$ values give straight lines with the slope $1/\varepsilon$ and intercept $1/K\varepsilon$ as shown in Fig. 4.

The oscillator strengths f were obtained from the following formula [25]:

$$f = (4.319 \times 10^{-9}) \varepsilon_{\max} \nu_{1/2}, \quad (2)$$

where $\nu_{1/2}$ is half-width of the band. The obtained parameters are given in Table 2. The [(FXN)(π -acceptors)] complexes have high complexation constants (K) and extinction coefficients (ε). High values of K reflect high stability of the complexes. The transition dipole moment (μ) of complexes were calculated by Eq. (3) [26]:

$$\mu = 0.0958 [\varepsilon_{\max} \nu_{1/2} / \nu_{\max}]^{1/2}, \quad (3)$$

where $\nu_{1/2}$ is halfwidth of the band, ε_{\max} and ν_{\max} are the extinction coefficient and wavenumber at the maximum of the peak. The ionization potential (I_p) of

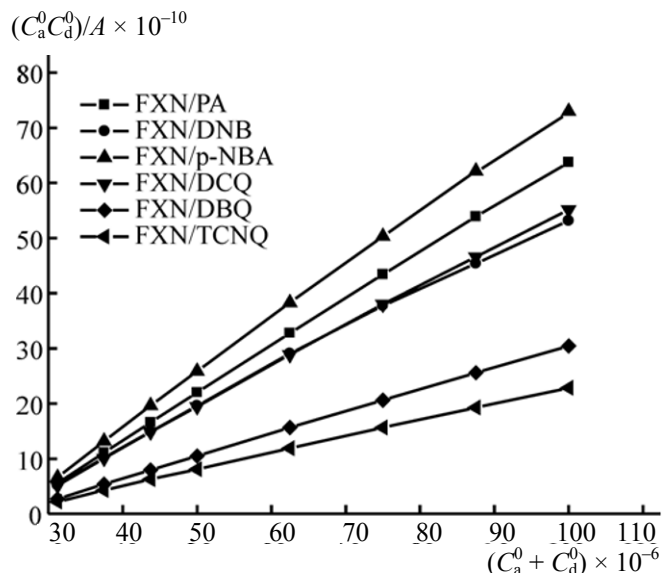


Fig. 4. The modified Benesi-Hildebrand plots for the FXN CT complexes in methanol.

free FXN was determined from the CT energies of the CT band of its complexes with different π -acceptors using the following relationships [27, 28]:

$$I_d (\text{eV}) = 5.76 + 1.53 \times 10^{-4} \nu_{\text{CT}}, \quad (4)$$

where E_{CT} is the energy of the CT of the FXN complex, the energy of the π - π^* or n - π^* interaction (E_{CT}) is calculated using Eq. (5) [26]:

$$E_{\text{CT}} (\text{eV}) = (h\nu_{\text{CT}}) = 1243.667/\lambda_{\text{CT}} (\text{nm}), \quad (5)$$

where λ_{CT} is the wavelength of the CT complex band. The resonance energy (R_N), was obtained from Eq. (6)

$$\varepsilon_{\max} (\text{L mol}^{-1} \text{ cm}^{-1}) = 7.7 \times 10^{-4} [h\nu_{\text{CT}}/(R_N) - 3.5], \quad (6)$$

where ε_{\max} is the molar extinction coefficient at the maximum, ν_{CT} is the frequency of the CT peak, and R_N

Table 2. Parameters of the FXN CT complexes in methanol

Sample	λ_{\max} , nm	E_{CT} , eV	K , L mol ⁻¹	ε_{\max} , L mol ⁻¹ cm ⁻¹	f	μ	I_p	D	R_N	$\Delta G^0(25^\circ\text{C})$, kJ/mol
PA	441	2.82	20000	24000	1.0	31.17	9.23	33	0.42	-24541
DNB	348	3.57	23000	29000	1.3	30.43	10.16	33	0.58	-24887
P-NBA	395	3.15	22000	20500	0.9	27.26	9.63	33	0.43	-24777
DCQ	516	2.41	21400	28000	1.2	36.41	8.72	33	0.39	-24709
DBQ	531	2.34	21000	50000	2.2	49.36	8.64	33	0.46	-24662
TCNQ	412	3.02	25500	13400	0.6	22.51	9.47	33	0.33	-25143

Table 3. Assignments of the IR spectral bands (cm^{-1}) of FXN and [(FXN)(π -acceptor)] charge transfer complexes

FXN	[(FXN)(acceptor)] CT-complexes						Assignments
	PA	DNB	<i>p</i> -NBA	DCQ	DBQ	TCNQ	
3500	—	—	—	—	—	—	$\nu_{\text{N-H}}$
3100	3086	3098	2964	3122	3122	3135	$\nu_{\text{C-H}}$; aliphatic
2925	2958	2958	2793	2964	3025	3049	$\nu_{\text{C-H}}$; aromatic
2854	2793	2793	2726	2793	2958	2970	
		2726		2732	2787	2787	
					2732	2738	
—	2446	—	2452	2452	2440	2452	Hydrogen bonding
	2379			2373	2373		
—	—	—	—	—	—	2220	$\nu_{\text{C}\equiv\text{N}}$
—	—	1708	1696	1751	1751	—	$\nu_{\text{C=O}}$; <i>p</i> -NBA, DCQ, DBQ
				1678	1678		
1651	1629	1617	1611	1617	1611	1611	δ_{NH} ; $-\text{NH}-\text{CH}_3$
1590	1556	1544	1537	1569	1574	1550	$\nu_{\text{C=C}}$
1517	1428	1470	1512	1511	1510		C-H deformation
1457		1410	1470	1477	1470		$\nu_{\text{as}}(\text{NO}_2)$
			1420	1404	1398		
1377	1331	1349	1337	1331	1331	1324	$\nu_{\text{C-N}}$
1329	1269	1288	1246	1239	1239	1246	$\nu_{\text{C-C}} + \nu_{\text{C-O}} + \nu_{\text{C-F}}$
1242	1239	1245	1166	1169	1160	1166	$\nu_{\text{s}}(\text{NO}_2)$
1184	1160	1166					CH, in-plane bend
1162							
1108	1117	1111	1111	1111	1117	1117	CH-deformation
1070	1069	1074	1068	1062	1069	958	$\nu_{\text{C-F}}$
1040	904	1038	1045	952	843	861	
1025	842	958	958	897	757	764	
1011	794	916	910	849			
958	745	830	880	764			
915		770	837				
904		721	764				
842							
819							
766							
700	703	703	703	697	703	696	skeletal vibration
649	642	642	642	641	636	641	CH bend
636	593	593	587	587	593	575	CH out of plane bend
624	514	532	520	520	514		CNC def.
596							$\delta(\text{NO}_2)$
566							
522							
475							

is the resonance energy of the complex in the ground state. The values of R_{N} for FXN/ π -acceptors complexes are given in Table 2. The standard free energy of complexation (ΔG^0) was calculated as $\Delta G^0 = -2.303 RT \log K_{\text{CT}}$.

Infrared spectra. The IR spectra of the CT complexes and the assignment of the bands [30] are given in Table 3. The observed changes on going from free reagents to their complexes can be assigned to the charge transfer from FXN to the π -acceptors and summarized as follows:

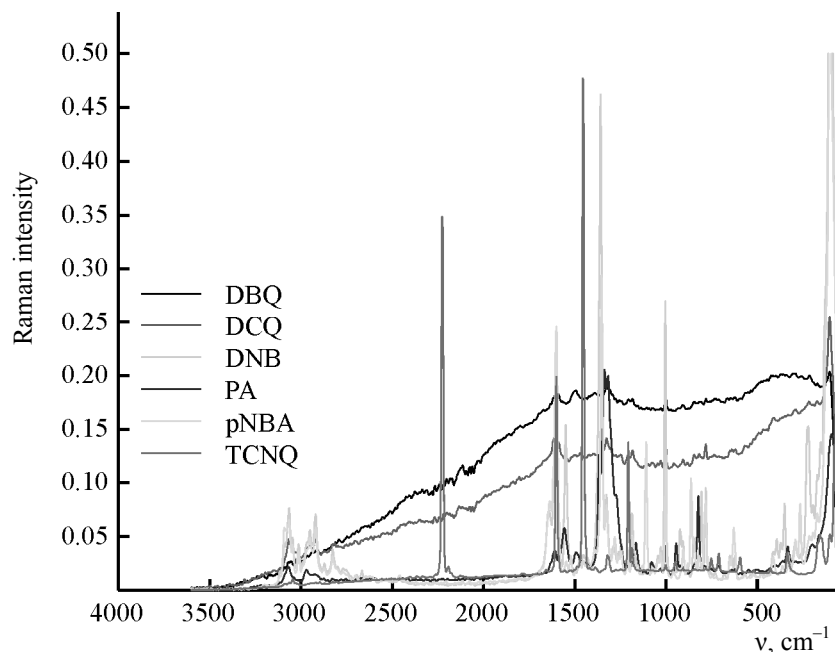


Fig. 5. Raman laser spectra of [(FXN)(π -acceptor)] charge transfer complexes.

(1) The absence in the complexes of specific $\nu(\text{NH})$ band at $\sim 3500 \text{ cm}^{-1}$ (free FXN) and the shift of the δ_{NH} band from 1651 cm^{-1} in FXN to lower wavenumbers ($1611\text{--}1629 \text{ cm}^{-1}$).

(2) The shift of the $\nu_{\text{C}=\text{C}}$ band from 1590 in the free FXN to $1569\text{--}1537 \text{ cm}^{-1}$ in the complexes and of the δ_{CH} bands from 1517 to $1512\text{--}1428 \text{ cm}^{-1}$.

(3) The shift of the $\nu_{\text{C}-\text{N}}$ from 1377 in the free FXN to $1349\text{--}1324 \text{ cm}^{-1}$ in its complexes.

(4) The presence of medium-to-weak bands at $2373\text{--}2452 \text{ cm}^{-1}$ in the spectra of complexes, which can be attributed to the stretching vibration of the intermolecular hydrogen bond of the NH proton of FXN [30]. The shift of the IR bands of the acceptor part to lower wavenumbers and those of the donor part to higher values reflects a donor to acceptor charge transfer of $\pi\text{--}\pi^*$ interaction, $D_{\text{HOMO}} \rightarrow D_{\text{LUMO}}$ transition [31].

The stoichiometry of the reaction between FXN and the studied π -acceptors was investigated by molar ratio method, which showed it to be 1: 1.

Raman spectra. Raman laser spectroscopy (Fig. 5) is complementary to the IR spectroscopy, which in turn emphasizes the charge transfer places of [(FXN)(π -acceptor)] complexes:

(1) The ν_{NH} and δ_{NH} bands are absent or shifted to lower frequencies ($1600\text{--}1608 \text{ cm}^{-1}$) in the FXN

complexes, which is consistent with participation of the NH group in the CT complexes with π -acceptors.

(2) The $\nu_{\text{C}=\text{C}}$ and δ_{CH} bands of the aromatic rings in FXN are shifted in the CT complexes to lower frequencies at $1569\text{--}1537$ and $\sim 1490 \text{ cm}^{-1}$, respectively.

(3) The $\nu_{\text{C}-\text{N}}$ bands are shifted to $1365\text{--}1325 \text{ cm}^{-1}$ in the complexes.

It should be noted that, unlike the spectra of other complexes, those with DCQ and DBQ are strongly broadened (Fig. 5), so that no reliable analysis for these two complexes is possible.

^1H NMR spectra. The ^1H NMR spectrum of free FXN hydrochloride contains a set of signals of aromatic protons in the range $7.0\text{--}7.8 \text{ ppm}$. The OCH proton appears as a triplet at 5.20 ppm . The NCH_2 and CCH_2 protons appear as the corresponding multiplets at 2.68 and 2.07 ppm , and the NMe group gives a singlet at 2.43 ppm .

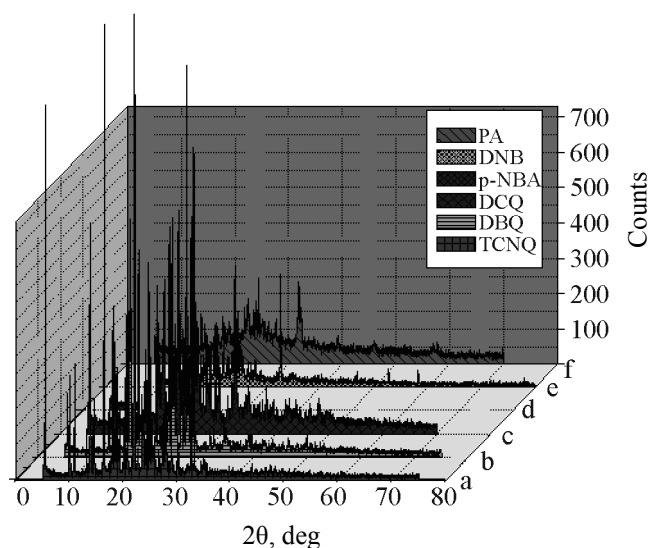
The chemical shifts (δ) of the protons in the spectra of the [(FXN)(π -acceptor)] CT complexes are listed in Table 4. All signals in the spectra of complexes are shifted downfield with respect to free FXN due to complex formation. The NH signal appears at $9.11\text{--}9.58 \text{ ppm}$, also due to the complex formation.

Scanning electron microscopy, EDX, and XRD studies. The surface morphology and crystalline

Table 4. Assignments of the ^1H NMR signals of the CT transfer complexes with FXN

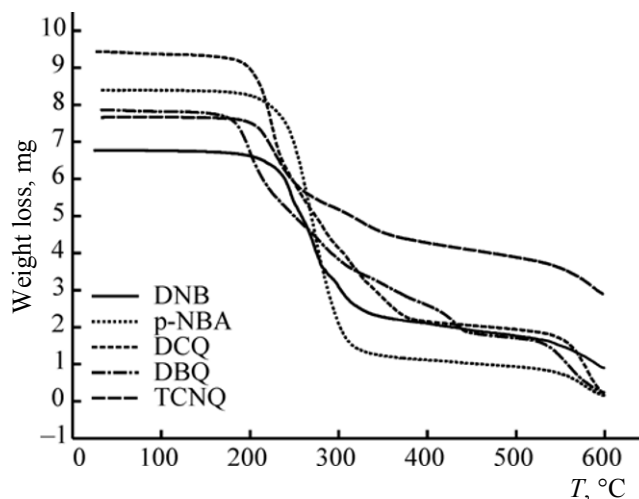
Group	CT complexes					
	PA	DNB	<i>p</i> -NBA	DCQ	DBQ	TCNQ
Aromatic	6.90–8.79	6.96–7.75	6.93–8.28	6.75–7.64	6.90–7.71	6.97–7.76
OCH	5.48–5.50	5.56	5.51–5.52	5.55, 5.76	5.56	5.56–5.58
NCH ₂	3.17–3.58	3.11–4.06	3.12–3.48	3.12–3.81	3.13–3.86	3.09–3.21
NMe	2.59–2.70	2.59–2.65	2.60–2.66	2.53–2.65	2.59–2.65	2.58–2.65
CCH ₂	2.31–2.41	2.38–2.47	2.41–2.49	2.39–2.43	2.39–2.45	2.36–2.43

structure of the synthesized CT complexes was analyzed by electronic microscopy SEM, EDX and XRD. The electron micrograph shows that the morphology of different FXN CT complexes depends on the acceptor. The EDX spectra corroborate the presence of carbon, oxygen, halogens (Cl and F) in the adducts. The uniformity and similarity of the particle forms of the synthesized complexes indicate that morphological phases of all complexes have a homogeneous matrix with the particle size in the range 50–500 μm . XRD patterns of some complexes are shown in Fig. 6. The peaks at $2\theta = 5^\circ$ and 80° are more target for the calculation of particle size using reflection from the XRD pattern by the Debye-Scherrer equation $D = 0.94\lambda/\beta\cos\theta$, where D is size of the particles, λ is the wavelength of X-ray, β is the full width at half maximum (FWHM), and θ is the angle [32]. The particles have the size within the range 50–300 nm.

**Fig. 6.** XRD spectra of [(FXN)(π -acceptor)] CT complexes.

Thermal and kinetic thermodynamic assessments.

The TG–DTG curves corresponding to the DNB complex heated in the 30–600°C temperature range are shown in Fig. 7. The thermal decomposition of [(FXN)(DNB)] complex has one strong broad peak recorded in DTG curve at $\text{DTG}_{\text{max}} = 251^\circ\text{C}$. This step is endothermic and assigned to the loss of organic moieties of FXN and DNB with weight loss 85.6% and the main residual is few carbon atoms. Thermal analysis of the [(FXN)(*p*-NBA)] complex confirmed the thermal stability and the number of degradation steps. According to TG and DTG profiles (Fig. 7) this step includes at least two decomposition steps at $\text{DTG}_{\text{max}} = 270$ and 568°C , both of them endothermic due to starting of melting and decomposition processes corresponding to the complete decomposition of FXN donor and *p*-NBA acceptor with weight loss 94.83%. Thermogravimetric analysis of the DCQ complex within the temperature range of 30–600°C showed one strong broad band and four

**Fig. 7.** TG curves of [(FXN)(π -acceptor)] CT complexes.

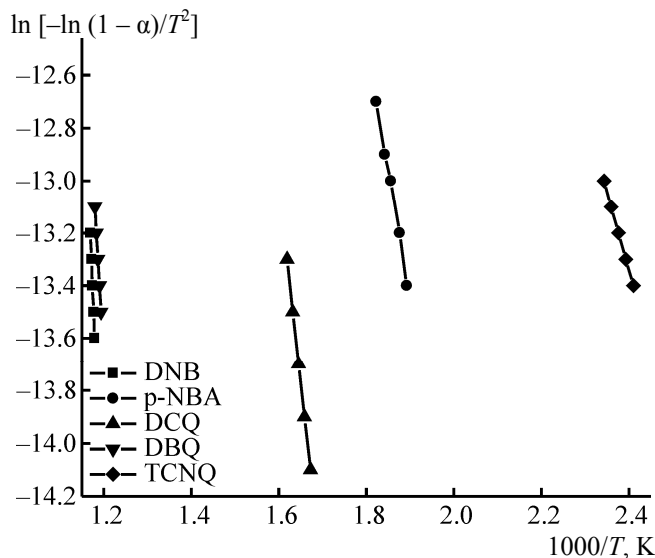


Fig. 8. Plots of Coats–Redfern relation for FXN CT complexes.

medium-to-weak degradation bands at 221, 278, 314, 354, and 575°C. These steps are endothermic and correspond to the loss of organic moieties of FXN and DCQ with weight loss 93.93% and the main residual is few carbon atoms. Thermal degradation of [(FXN)(DBQ)] complex has four steps at 199, 279, 417, and 556°C, also corresponding to the completely decomposition with weight loss 96.13%. The TCNQ complex in the 30–600°C range has three peaks at 228, 322, and 567°C corresponding to the loss of organic moieties of FXN and TCNQ with weight loss 62.09% and the main residual is few carbon atoms. The analysis of the thermal decomposition curves gives the following order of stability of the CT complexes: *p*-NBA > DNB > TCNQ > DCQ > DBQ.

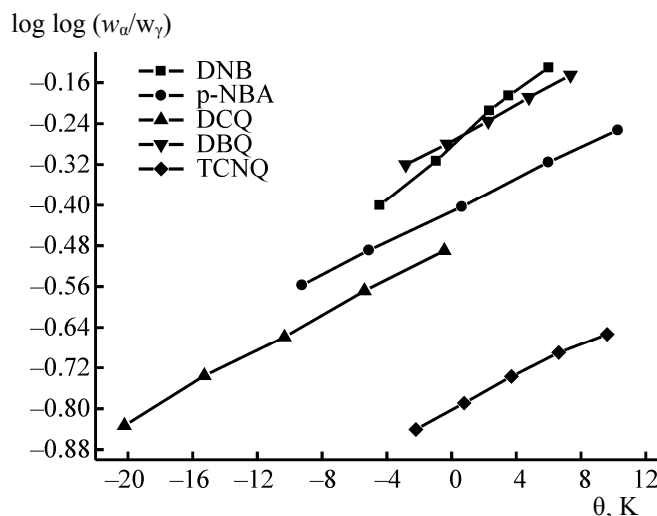


Fig. 9. Plots of Horowitz–Metzger relation for FXN CT complexes.

This sequence can be discussed according to the accepting powerful of *p*-NBA and DNB that contain nitro groups as strong electron acceptors. The [(FXN)(TCNQ)] complex could not be analyzed because of its explosive properties.

Many works deal with determining the rate-dependent parameters of solid-state non-isothermal decomposition reactions by analysis of TG curves. Several equations [33–35] have been proposed for calculation of the kinetic parameters. Two major methods, the Horowitz–Metzger approximation method [34] and the Coats–Redfern integral method [35] are used for evaluation of kinetic parameters. The enthalpy of activation ΔH and the free enthalpy of activation ΔG can be calculated via Eq. (7).

Table 5. Kinetic parameters calculated from Coats–Redfern (CR) and Horowitz–Metzger (HM) equations

Complex stage	Method	Parameter					<i>r</i>
		<i>E</i> , J/mol	<i>A</i> , s ^{−1}	ΔS , J mol ^{−1} K ^{−1}	ΔH , J/mol	ΔG , J/mol	
FXN/DNB	CR	3.51×10^5	3.88×10^{19}	1.18×10^2	3.38×10^5	2.35×10^5	0.9958
	HM	3.64×10^5	5.50×10^{20}	1.33×10^2	3.55×10^5	2.32×10^5	0.9990
FXN/ <i>p</i> -NBA	CR	7.30×10^4	1.51×10^5	-1.50×10^2	7.30×10^4	1.61×10^5	0.9980
	HM	8.60×10^4	1.34×10^5	-1.36×10^2	8.10×10^4	1.50×10^5	0.9979
FXN/DBQ	CR	2.30×10^5	3.22×10^{12}	-1.45×10^1	2.22×10^5	2.35×10^5	0.9995
	HM	2.34×10^5	2.11×10^{12}	-1.73×10^1	2.23×10^5	2.34×10^5	0.9993
FXN/DCQ	CR	5.10×10^4	5.00×10^3	-1.76×10^2	4.65×10^4	1.20×10^5	0.9995
	HM	5.80×10^4	1.55×10^5	-1.44×10^2	5.45×10^4	1.15×10^5	0.9979
FXN/TCNQ	CR	7.88×10^4	2.14×10^4	-1.65×10^2	7.33×10^4	1.69×10^5	0.9860
	HM	8.70×10^4	2.01×10^5	-1.50×10^2	8.31×10^4	1.70×10^5	0.9990

$$\Delta H = E - RT_m; \Delta G = \Delta H - T_m \Delta S. \quad (7)$$

The kinetic parameters evaluated graphically using the two above-mentioned methods are listed in Table 5. High correlation coefficients (~ 1) in all cases indicate a good agreement with the experiment and prove the reliability of the calculated kinetic parameters. The calculated of activation energy ΔE^* values using both methods for the main decomposition step of the FXN CT complexes are as follows: TCNQ (829 kJ/mol) > *p*-NBA (795 kJ/mol) > DBQ (545 kJ/mol) > DNB (358 kJ/mol) > DCQ (232 kJ/mol), in accordance with the electron acceptor power of the acceptor. The negative values of ΔS^* (Table 5) are typical for the adduct formation reactions.

CONCLUSIONS

The interactions of the electron donor fluoxetine hydrochloride drug with π -acceptors picric acid, dinitrobenzene, *p*-nitrobenzoic acid, 2,6-dichloroquinone-4-chloroimide, 2,6-dibromoquinone-4-chloroimide, 7,7',8,8'-tetracyanoquinodimethane were studied spectrophotometrically in methanol. New charge-transfer 1 : 1 complexes were isolated and characterized by spectroscopic methods and thermogravimetric analysis. The formed CT-complexes have the formulas [(FXN)(π -acceptors)].

ACKNOWLEDGMENTS

This work was supported by grants from Princess Nora Bint Abdul Rahman University, Riyadh, Saudi Arabia under project Grants no. 25/32.

^1H NMR, IR spectra, SEM images can be requested from the authors.

REFERENCES

1. "Prozac Pharmacology, Pharmacokinetics, Studies, Metabolism," RxList.com, 2007, recieved April 14, 2007.
2. Bueno, F., Bergold, A.M., and Fröhlich, P.E., *Bollettino Chimico Farmaceutico*, 2000, vol. 139, no. 6, p. 256.
3. Shamsipur, M., Dastjerdi, L.S., Haghighi, S., Armspach, D., Matt, D., and Aboul-Enein, H.Y., *Anal. Chim. Acta*, 2007, vol. 601, no. 1, p. 130.
4. Atta-Politou, J., Skopelitis, I., Apatsidis, I., and Koupparis, M., *Eur. J. Pharm. Sci.*, 2001, vol. 12, no. 3, p. 311.
5. Shah, C.R., Shah, N.J., Suhagia, B.N., and Patel, N.M., *J. AOAC Int.*, 2007, vol. 90, no. 6, p. 1573.
6. Nevado, J. J. B., Llerena, M.J.V., Cabanillas, C.G., Robledo, V.R., and Buitrago, S., *J. Separ. Sci.*, 2006, vol. 29, no. 1, p. 103.
7. Mandrioli, R., Pucci, V., Visini, D., Varani, G., and Raggi, M.A., *J. Pharm. Biomed. Anal.*, 2002, vol. 29, no. 6, p. 1127.
8. Darwish, I.M., Refaat, I.H., Askal, H.F., and Marzouq, M.A., *J. AOAC International*, 2006, vol. 89, no. 2, p. 334.
9. Darwish, I.A., Amer, S.M., Abdine, H.H., and Al-Rayes, L.I., *J. Fluorescence*, 2009, vol. 19, no. 3, p. 463.
10. Roy, D.K., Saha, A., and Mukherjee, A.K., *Spectrochim. Acta A*, 2005, vol. 61, p. 2017.
11. Hamed, M.M.A., Abdel-Hamid, M.I., and Mahmoud, M.R., *Monatsh. Chem.*, 1998, vol. 129, p. 121.
12. Dozal, A., Keyzer, H., Kim, H.K., and Way, W.W., *Int. J. Antimicrob. Agent*, 2000, vol. 14, p. 261.
13. Refat, M.S., El-Zayat, L.A., and Yeşilel, O.Z., *Spectrochim. Acta Part A*, 2010, vol. 75, p. 745.
14. Pandeewaran, M., and Elango, K.P., *Spectrochim. Acta Part A*, 2009, vol. 72, p. 789.
15. Al-Attas, A.S., Habeeb, M.M., and Al-Raimi, D.S., *J. Mol. Liquid*, 2009, vol. 148, p. 58.
16. Lee, S.R., Rahman, M.M., Sawada, K., and Ishida, M., *Biosens. Bioelectron.*, 2009, vol. 24, p. 1877.
17. Attama, A.A., Nnamani, P.O., Adikwu, M.U., and Akidi, F.O., *Chem. Pharm. Bull.* 2004, vol. 52(3), p. 303.
18. Askal, H.F., *Talanta*, 1997, vol. 44, no. 10, p. 1749.
19. Sharma, K., Sharma, S.P., and Lahiri, S.C., *Spectrochim. Acta Part A*, 2012, vol. 92, no. 15, p. 212.
20. Ganesh, K., Balraj, C., Satheshkumar, A., and Elango, K.P., *Spectrochim. Acta Part A*, 2012, vol. 92, no. 15, p. 46.
21. Ganesh, K., and Elango, K.P., *Spectrochim. Acta Part A*, 2012, vol. 93, p. 185.
22. Refat, M.S., Saad, H.A., and Adam, A.A., *J. Mol. Str.*, 2011, vol. 995, no. 1-3, p. 116.
23. Skoog, D.A., *Principle of Instrumental Analysis*, 3 ed., Saunders College Publishing, New York, USA, 1985, ch. 7.
24. Abu-Eittah, R. and Al-Sugeir, F., *Can. J. Chem.*, 1976, vol. 54, p. 3705.
25. Tsubomura, H. and Lang, R.P., *J. Am. Chem. Soc.*, 1964, vol. 86, p. 3930.
26. Rathone, R., Lindeman, S.V., and Kochi, J.K., *J. Am. Chem. Soc.*, 1997, vol. 119, p. 9393.
27. Briegleb, G., *Z. Angew. Chem.*, 1964, vol. 76, p. 326.
28. Aloisi, G., and Pignataro, S., *J. Chem. Soc. Faraday Trans.*, 1972, vol. 69, p. 534.
29. Briegleb, G., and Czekalla, J., *Z. Physikchem. (Frankfurt)*, 1960, vol. 24, p. 237.
30. Bellamy, L.J., *The Infrared Spectra of Complex Molecules*, London: Chapman & Hall, 1975.
31. Foster, R., *Organic Charge-Transfer Complexes*, New York: Academic Press, USA, 1969.
32. Guinier, A., *X-Ray Diffraction*, San Francisco, 1963.
33. Freeman, E.S., and Carroll, B., *J. Phys. Chem.*, 1958, vol. 62, p. 91.
34. Horowitz, H.H., and Metzger, G., *Anal. Chem.*, 1963, vol. 35, p. 1464.
35. Coats, A.W. and Redfern, J.P., *Nature*, 1964, vol. 201, p. 68.